Clim Dyn (2018) 50:2157–2168
DOI 10.1007/s00382-017-3741-7

Regional difference of the start time of the recent warming in Eastern China: prompted by a 165-year temperature record deduced from tree rings in the Dabie Mountains

Qiufang Cai[1] · Yu Liu[1,2] · Bingchuang Duan[1,3] · Changfeng Sun[1,2]

Received: 24 December 2016 / Accepted: 24 May 2017 / Published online: 1 June 2017

Abstract Tree-ring studies from tropical to subtropical regions are rarer than that from extratropical regions, which greatly limit our understanding of some critical climate change issues. Based on the tree-ring-width chronology of samples collected from the Dabie Mountains, we reconstructed the April–June mean temperature for this region with an explained variance of 46.8%. Five cold (1861–1869, 1889–1899, 1913–1920, 1936–1942 and 1952–1990) and three warm (1870–1888, 1922–1934 and 2000–2005) periods were identified in the reconstruction. The reconstruction not only agreed well with the instrumental records in and around the study area, but also showed good resemblance to previous temperature reconstructions from nearby regions, indicating its spatial and temporal representativeness of the temperature variation in the central part of eastern China. Although no secular warming trend was found, the warming trend since 1970 was unambiguous in the Dabie Mountains (0.064 °C/year). Further temperature comparison indicated that the start time of the recent warming in eastern China was regional different. It delayed gradually from north to south, starting at least around 1940 AD in the north part, around 1970 AD in the central part and around 1980s in the south part. This work enriches the high-resolution temperature reconstructions in eastern China. We expect that climate warming in the future would promote the radial growth of alpine *Pinus taiwanensis* in the subtropical areas of China, therefore promote the carbon capture and carbon storage in the *Pinus taiwanensis* forest. It also helps to clarify the regional characteristic of recent warming in eastern China.

Keywords Subtropical area · Tree-ring width · Temperature reconstruction · Spatial representativeness · Eastern China · Regional difference of recent warming

1 Introduction

Global warming (GW) is not only changing the ecological process of the world, but also human activities, threatening food sources vital to local people (Walther et al. 2002; Cohen et al. 2016; Crabbe et al. 2016). The effect of GW may be spatially inhomogeneous (IPCC 2007; Yadav and Singh 2002; Xing et al. 2014). Therefore, studying the regional characteristics of GW is meaningful not only for the ecological safety, but also for the social and economic development.

As the main indicator of GW, temperatures on different spatial and temporal scale have been reconstructed around the world by using various paleoclimatic proxies (Ljungqvist 2010; Linderholm et al. 2015). High-resolution tree rings, containing rich climate information (Fritts 1976; Liang et al. 2008), are the dominant data type in most continental/hemispheric temperature reconstructions (Moberg et al. 2005; Shi et al. 2015a). However, tree-ring materials adopted in these researches are mainly from mid-high

✉ Qiufang Cai
caiqf@ieecas.cn

✉ Yu Liu
liuyu@loess.llqg.ac.cn

[1] The State Key Laboratory of Loess and Quaternary Geology, The Institute of Earth Environment, Chinese Academy of Sciences, 97 Yanxiang Road, Yanta District, Xi'an 710061, China

[2] Department of Earth and Environment Science, School of Human Settlements and Civil Engineering of Xi'an Jiaotong University, Xi'an 710049, China

[3] The University of the Chinese Academy of Science, Beijing 100049, China

latitudes (Esper et al. 2002; Christiansen and Ljungqvist 2012), studies from the tropical to subtropical regions are lacking. In China, tree-ring based temperature reconstructions are also inhomogeneous due to the diverse landforms and the inhomogeneous distribution of forests. Significant progress has been achieved in comparatively dry regions (Gou et al. 2008; Cai et al. 2014), around the Tibetan Plateau in particular (Yang et al. 2010; Zhang et al. 2015; Yin et al. 2016). Studies in the subtropical areas of China (Chen et al. 2012a; Duan et al. 2012) are relatively underdeveloped so far, which greatly limit our fully understanding of some critical climate issues. Although temperature variation in China have been discussed in various scientific literatures, topics about the spatial–temporal characteristics of the recent warming were mostly focused on the intensity and seasonality (Qian and Qin 2006; Ling et al. 2012; Wang et al. 2012; Guan et al. 2015), very few on the timing and regional difference. Considering the previous studies were mainly based on short instrumental data, the analyses from long-time scale tree rings are urgently needed.

In this paper, we present a new case study to show the potential of using tree rings for temperature reconstruction in subtropical eastern China. We aim to evaluate the temperature effect on tree growth, to reconstruct the temperature history during the initial stage (April–June) of tree growth. Both the credibility and spatial and temporal representativeness of the reconstruction are therefore tested. On the basis of our new reconstruction and other existing temperature records inferred from tree rings from eastern China (EC >100°E), we tentatively analyzed the regional difference of the start time of recent decades warming in EC.

2 Materials and methods

2.1 Tree-ring data

As a key mountain range in central EC, the Dabie Mountains (30°00′–32°30′N, 112°40′–117°10′E) extend approximately 270 km from northwest to southeast and separate two major rivers in China, Huai and Yangtze river. The mountains also form a natural boundary between Hubei and its two neighboring provinces, Henan in the north and Anhui in the east. The eastern part of the mountains is generally over 1000 m a.s.l., higher than the western part (300–400 m a.s.l.). Baima peak (1777 m a.s.l.) and Tiantangzhai (TTZ, 1729.13 m a.s.l.) are the first and second peaks of this mountain range, respectively.

In May, 2012, 54 tree-ring cores were collected from 27 healthy *Pinus taiwanensis* Hayata at the elevation around 1550 m a.s.l. from TTZ (31.11–31.12°N, 115.7–115.8°N, Fig. 1), with two cores from each tree. TTZ has been hailed as the last piece of virgin forest in east China. At the low part of TTZ, *Pinus taiwanensis* is mixed with young *Lindera rubronervia* Gamble, *Quercus aliena* Bl., Indocalamus longiauritus Hand.-Mazz. and *Coriaria nepalensis Wall*. At the sampling site, the forest is composed of pure

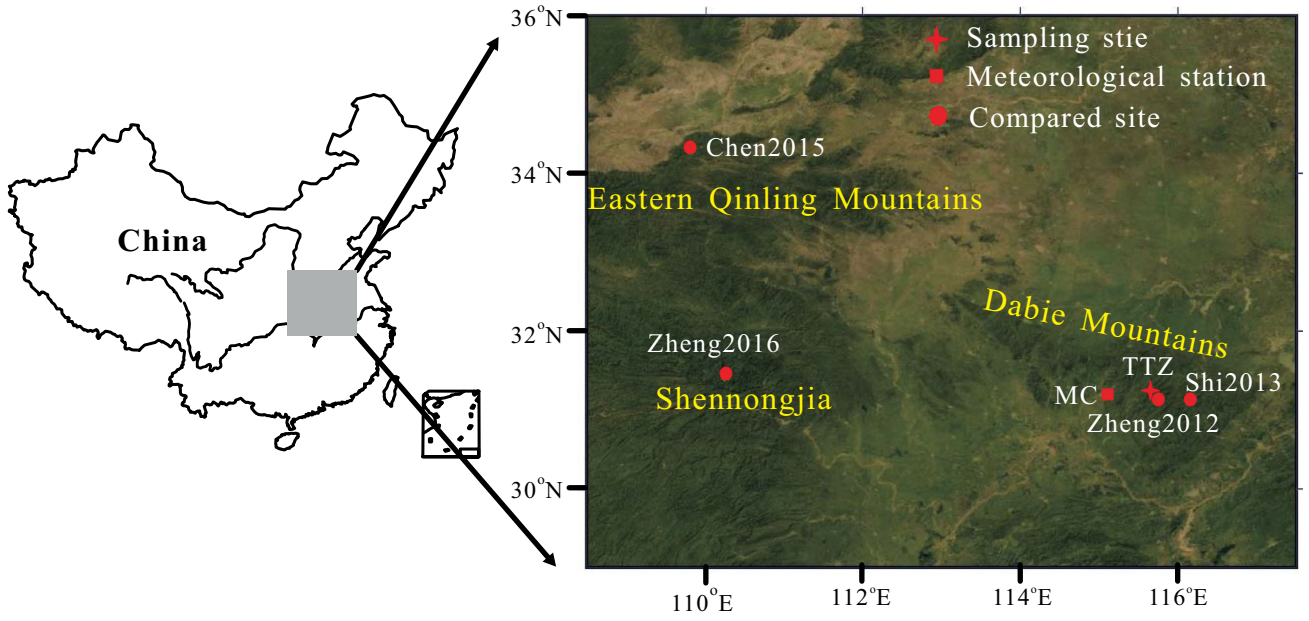

Fig. 1 Positions of the Macheng meteorological station (MC), the sampled site in Tiantangzhai (TTZ) and sites used for comparison in the Dabie Mountains (Zheng 2012: Zheng et al. 2012; Shi 2013: Shi et al. 2013), Eastern Qinling Mountains (Chen 2015: Chen et al. 2015) and the Shennongjia region (Zheng 2016: Zheng et al. 2016)

Pinus taiwanensis with very open canopy. The sampled tree grew on the edge of the cliff with thin layer of yellow–brown mountain soil.

Following the standard method of pretreatment (Cook and Kairiukstis 1990), all the samples were fixed on the wooden trough, sanded with sand papers of different mesh until the surfaces were smooth and the ring boundaries were clear and distinguishable under the microscope. The cores were visually dated and then measured using the LINTAB measurement machine with precision up to 0.01 mm. Afterwards, the COFECHA program (Holmes 1983) was applied for evaluating the quality of measurements and crossdating, to exclude the possibility of false rings or missing rings. This procedure assures the accuracy of the calendar year of each ring. The tree-ring-width measurement series that have successfully passed the COFECHA program were therefore combined to develop the tree-ring chronology via the ARSTAN program (Cook 1985). For the removal of non-climate signal caused by the Juvenile effect (Fritts 1976), each tree-ring series was corrected with negative exponential curve or straight line. Namely, a dimensionless index for each tree-ring core was computed by dividing the original measurement of each ring by the value of the fitted curve in the corresponding year. Then all the dimensionless indexes were combined into a single standard (STD) chronology by computing a biweight robust mean (Cook 1985). The STD chronology (Fig. 2) was therefore adopted in the following analysis because it contained both high- and low-frequency signals. The mean series length of all the samples is 121.6 year, so the STD chronology should preserve variability on time scale up to 41 year (Cook et al. 1995). The SSS method (subsample signal strength), introduced by Wigley et al. (1984), was adopted to ascertain the reliable starting year of the chronology, excluding the early period with low sample size. Meanwhile, the statistical parameters were analyzed during the common period (1932–2007) to evaluate the quality of the chronology.

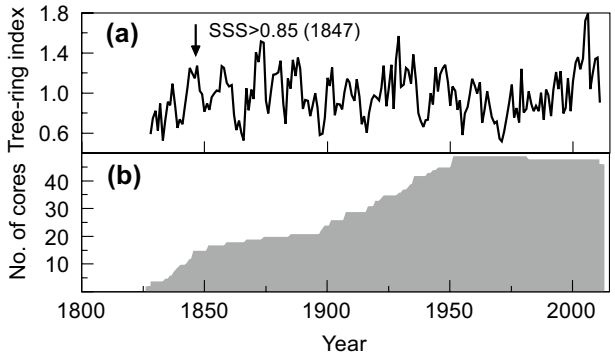

Fig. 2 Plots of **a** the STD chronology and **b** the sample depth

2.2 Climate data

Influenced by the East Asian monsoon system, the climate in this region is comparatively warm and humid, with typical mountainous climate characteristics and abundant precipitation. Monthly climate data including precipitation and temperature are extracted from the nearby meteorological station in Macheng (MC, 31°11′N, 115°01′E, 593 m a.s.l.). According to the records from this station, the mean annual precipitation and temperature are 1350 mm and 12.6 °C, respectively. The mean annual relative humidity is about 85%. January and July are the coldest (3.39 °C) and hottest (28.65 °C) months of the year, respectively (Fig. 3a). The months with precipitation more than 100 mm are from April to August, with July (232.92 mm) as the peak. During

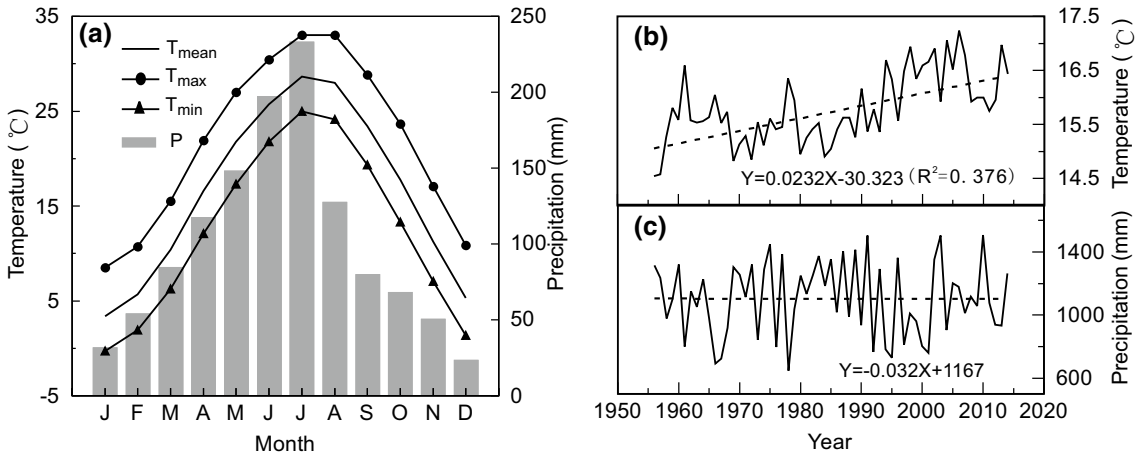

Fig. 3 Climatic records from the Macheng meteorological station. **a** Monthly maximum (T_{max}), mean (T_{mean}), minimum (T_{min}) temperatures and monthly precipitation (P); **b** multi-year averaged annual mean temperature and **c** mean annual total precipitation. *Dashed lines* indicate the linear trends

the instrumental period (1959–2014), the annual mean temperature indicates an increasing trend (Fig. 3b), most robust since around 1970, while no obvious long-term trend of annual total precipitation is seen (Fig. 3c).

2.3 Statistical methods

To determine whether the climate has impact on the radial growth of *Pinus taiwanensis*, and which climate factor limits tree growth most, Pearson correlation analysis was computed between the STD chronology and meteorological data. The analyses were based on monthly and seasonal (different combinations of consecutive months) climate data from prior January to current October, considering the lag-effect of climate (Fritts 1976). Since autocorrelations may exist in the data used in this study, it must be taken into account when we determine the significance of the correlations (Christiansen and Ljungqvist 2017). Therefore, the effective number of degree of freedom (*EDF*) was estimated according to the equation $EDF = N\left(1 - r_1 \times r_2\right)/\left(1 + r_1 \times r_2\right)$ (Shao et al. 2010), adjusted from (Bretherton et al. 1999). Where N is the number of observations, and r_1 and r_2 refer to the lag-one autocorrelation of each series, respectively. All the significance of correlations in the following analysis was based on *EDF*.

When the limiting climate factor was determined, the targeted climate factor was reconstructed. Different reconstruction method may have different influence on the preservation of low-frequency information (Christiansen and Ljungqvist 2017). In view of this study, it belongs to a single-site temperature reconstruction. We compared two reconstruction methods which are suitable for single-site reconstruction: direct regression and indirect regression (Christiansen 2011; Christiansen and Ljungqvist 2017). We found that there was some difference in the low-frequency signals between the two reconstructed results, but not obvious. Given that the direct regression method was widely used in single-site reconstructions (Duan et al. 2012; Liu et al. 2009a, b), and the reconstructed timeseries used in the following comparison were all based on direct regression method, the targeted climate factor in this study was therefore reconstructed by direct regression—a simple regression model using temperature as the dependent variable.

Jackknife (Efron 1979) and Bootstrap (Cook and Kairiukstis 1990) methods, recommended in previous dendroclimatological studies (Liu et al. 2009a; Zheng et al. 2012), were applied to evaluate the stability of the regression model. If the statistical parameters of these two methods were similar to that of the regression model, the model would be considered as stable, dependable and proper for further reconstruction. To test the large-scale representativeness of the reconstruction, spatial correlation maps for the April–June temperature were calculated via the website http://climexp.knmi.nl (van Oldenborgh et al. 2009). Additionally, temperature series from different parts of EC were further compared to identify the regional difference of the timing of the recent warming.

3 Results and discussions

3.1 The STD chronology

Totally, 47 ring-width measurement series passed the COFECHA program with high series intercorrelation ($r = 0.59$). The STD chronology was therefore established (1828–2011) based on the 47 measurement series, while the reliable chronology spanned from 1847 (SSS > 0.85) to 2011 (Fig. 2). During the common period (1932–2007), the correlation coefficient (r) within trees was 0.65, and 0.40 among all series. The high r values indicated that the tree-ring width series had similar yearly variation, which may be caused by similar external influence such as climate. The variance in first eigenvector was 44.50%. The expressed population signal (EPS), a measure of how well a chronology based on limited sample size approximates the theoretical chronology that has been infinitely replicated from the individual sample (Wigley et al. 1984; Cook and Kairiukstis 1990), was 0.92, better than the recommended threshold 0.85. These parameters further demonstrated the high quality of the tree-ring chronology in TTZ. Moreover, the first-order autocorrelation of the chronology was 0.56, suggesting that the lag-effect of climate influence on tree growth might exist in the study area.

3.2 Climate–growth relationship

The STD chronology at the high elevation of TTZ showed consistently positive relationships with almost all the monthly (mean, minimum and maximum) temperature records (Fig. 4). Significant correlations with temperature ($p < 0.05$) were found not only in current February–October, with the exception of May and August, but also in prior January–July and prior September ($p < 0.05$) (Fig. 4a). After combining the temperature records of different consecutive months, the STD chronology showed the most significant correlation with the February–July mean temperature in prior year (PT_{27}), with $r = 0.71$ ($EDF = 25$, $p < 0.01$). It also showed positive responses to the mean temperatures of different seasonal combinations from prior January to prior July and from current January to current July ($p < 0.01$) (Table 1). It demonstrated that the January–July temperature variations of both prior and current year significantly influenced the radial growth of *Pinus taiwanensis* at the high elevation area of the Dabie Mountains. In contrast,

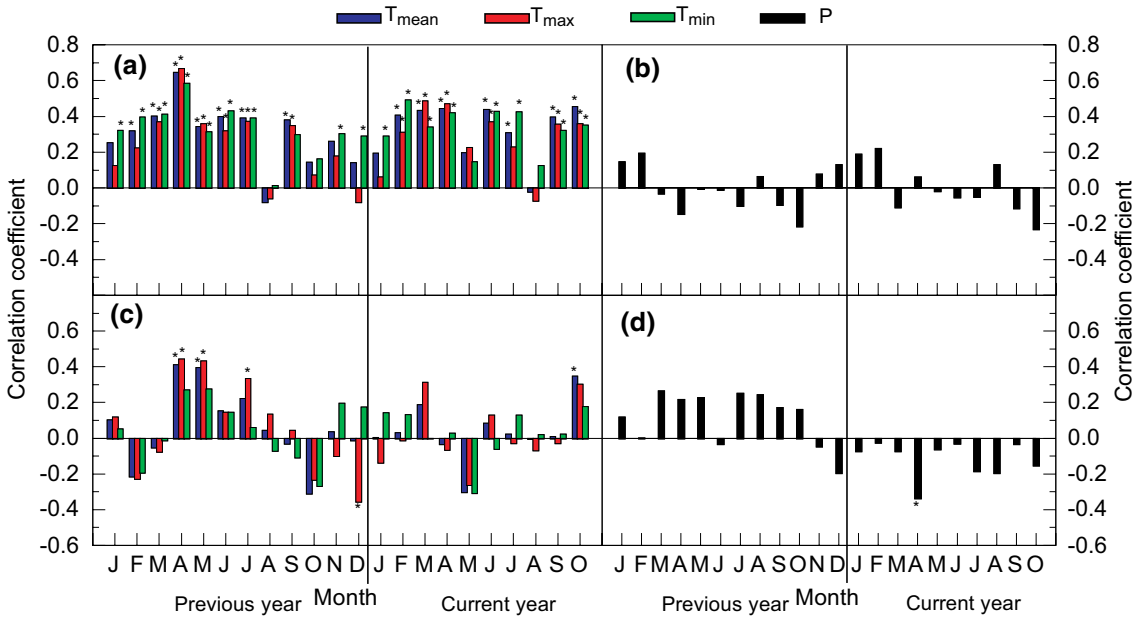

Fig. 4 Results of the correlation (**a, b**) and first-order difference correlation (**c, d**) between the STD chronology and monthly temperatures and precipitation over 1959–2011. *Asterisk* indicates that the correlation coefficient is above the 95% confidence level, which is based on the effective number of degree of freedom (*EDF*) described by Bretherton et al. (1999)

Table 1 Correlation coefficient (r) between the raw and first-order difference series (1st) of the tree-ring STD chronology and mean temperature of different seasonal combination

	PT_{17}	PT_{27}	PT_{37}	PT_{46}	CT_{17}	CT_{27}	CT_{37}	CT_{46}
r	0.70[a]	0.71[a]	0.69[a]	0.68[a]	0.63[a]	0.63[a]	0.57[a]	0.50[a]
r_{1st}	0.30	0.28	0.39	0.57[a]	−0.01	−0.01	0.02	−0.13

The numerical subscripts in the first line indicate different combinations of consecutive months, e.g. 17 means January–July mean temperature

PT prior year mean temperature, *CT* current year mean temperature

[a]Indicates the 99% confidence level based on the effective number of degree of freedom (*EDF*) described by Bretherton et al. (1999)

the tree rings did not show any significant responses to the monthly or seasonal precipitation (Fig. 4b).

At first glance, the above result was just similar to that of other previous studies in the Dabie Mountains by Zheng et al. (2012) and Shi et al. (2013). To further confirm such relationship, the first-order difference r values (r_{1st}) between the STD chronology and monthly/seasonal climatic factors were calculated (Fig. 4c, d). It indicated that the ring-width STD chronology still had significant relationship with the monthly mean temperatures in current October, prior April and prior May ($p<0.05$). Surprisingly, the tree rings did not show any significant relationship with the seasonal temperatures of the current year. On the contrary, tree rings kept positive correlations with the prior seasonal temperatures (Table 1), though the relationship with PT_{27} reduced sharply ($r=0.28$, $EDF=34$, $p<0.1$). At seasonal scale, the tree rings only showed significant correlation with prior April–June mean temperature (PT_{46}) with $r=0.57$ ($EDF=36$, $p<0.01$). The first-order difference correlation analysis revealed that the foregoing high r values (0.71, 0.70) between the tree rings and PT_{27} or PT_{17} (prior January–July mean temperature) were mostly caused by similar low-frequency trends. If we choose PT_{27} or PT_{17} for reconstruction, the high-frequency signal in the reconstruction will be unreliable. Considering to keep both the high- and low-frequency climate signals as much as possible, PT_{46} ($r=0.68$, $p<0.01$) will be the optimal choice.

April–June belongs to the early stage of growing season for trees in the subtropical area of China (He et al. 2012), which is crucial for the expansion of early wood. Ring width relies on the products of photosynthesis during the current growing season to provide the carbohydrate for tissues building. Warm climate is advantageous to the production of enzymes and hormones which are necessary for photosynthetic activity of trees. It promotes tree growth and produces wide rings. Inversely, low

temperature during April–June may limit tree growth and cause narrow rings. Moreover, high temperature during the early growing months favors meristematic activities of trees, which results in earlier growth and further prolongs growing season (Cai and Liu 2017). The climate-growth relationship in the Dabie Mountains is in accordance with the general assumption that tree rings at high elevation of the Mountains are more sensitive to temperature variation (D'Arrigo et al. 2001; Yin et al. 2016), due to the comparatively cold environment.

The stored carbohydrates during previous years are also a significant source for wood formation during the following growing season, particularly in the early stage (Campioli et al. 2011). The significant relationship between tree-ring growth and previous growing-season temperature could be explained as a carry-over effect caused by carbohydrate accumulation in warm (cold) years leading to a growing increment (reduction) in the subsequent year. Piovesan et al. (2008) even reported that the June–August summer temperature 2 years prior to tree growth had significantly positive correlation with the tree-ring chronology of *F. sylvatica* in Italy. A high temperature during the previous growing season can help trees produce and accumulate more photosynthate before dormancy in winter, which can be utilized at least partly by the formation and manufacture of the earlywood in the following growing seasons (McCarroll and Loader 2004; Ols et al. 2016). For example, when Skomarkova et al. (2006) studied the tree rings in *F. sylvatica*, they found that 10–20% ring width may be affected by the remobilized carbon of the tree formed in the previous growing seasons. Campioli et al. (2011) found that previous year temperature could explain about 50% of the net primary production (NPP)–gross primary production (GPP) variability in leaves and wood, respectively. During the early period of the growing season, the vast majority of GPP was allocated to leaf and stem NPP, and consequently influencing the carbon availability for the radial growth of trees (Campioli et al. 2011). The lag-effect of climate on trees, revealed in various species around the world (Liu et al. 2009a; Davi et al. 2015), is meaningful in tree physiology (Fritts 1976). In subtropical area of China, the lag-effect of climate on tree growth is particularly significant (Duan et al. 2012; Li et al. 2014; Cai and Liu 2017; Cai et al. 2016).

From Fig. 3b we can see that the warming trend in the Dabie Mountains is evident. We expect that climate warming in the future would promote the radial growth of alpine *Pinus taiwanensis* in the subtropical areas of China. In turn, the ongoing warming would possibly benefit the carbon capture and carbon storage (Melillo et al. 2011; Yu et al. 2016) in the *Pinus taiwanensis* forest.

3.3 PT_{46} reconstruction and characteristics

On the basis of the above consideration, we reconstructed PT_{46} instead of PT_{27}. The regression model was designed as: $PT_{46} = 2.045 \times STD_t + 19.28$ ($r = 0.68$, $r^2 = 46.80\%$, $r^2_{adj} = 45.70\%$, $F = 43.86$). STD_t in the function refers to the tree-ring index in the year t. The reconstruction can explain 46.80% variance of the observation during 1960–2011, 45.7% after adjustment for the loss of degrees of freedom. F value, a parameter that indicates the ratio of the variance of the regression model and residual error, was 43.86. Generally, the bigger the F value is, the smaller the residual error is, the better the accuracy of the simulation. Figure 5a illustrated that the reconstructed temperature had good skill in simulating the observed temperature. Moreover, the statistical results in Table 2 proved high skill of the regression model in imitating the observation.

The prior April–June mean temperature was therefore reconstructed back to 1847. The reconstructed temperature varied between 20.33 and 22.95 °C, with a mean value of 21.31 °C. The standard deviation (σ) of the reconstructed temperature was 0.48 °C. To facilitate the following discussion, we adjusted the time scale of the reconstruction with t − 1 to indicate the mean April–June temperature in the study area. Namely, we reconstructed the April–June mean temperature of Dabie Mountains from 1846 to 2010 (Fig. 5b).

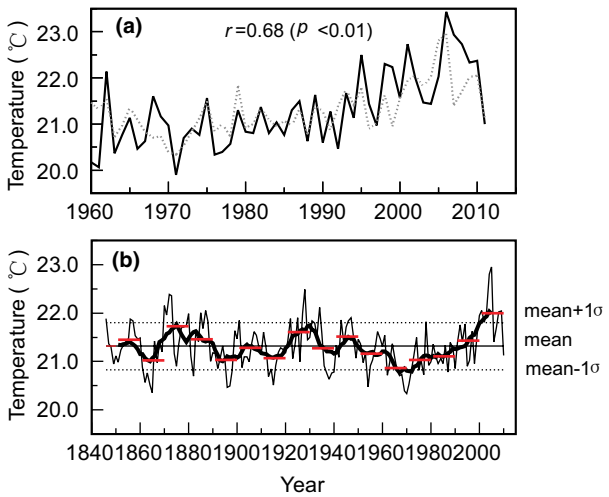

Fig. 5 **a** Prior April–June temperature comparison between the reconstruction (*gray dashed line*) and observation (*black line*) during 1960–2011. **b** The reconstructed April–June mean temperature in the Dabie Mountains during 1846–2010 (*thin grey curve*). The *thick curve* is the 11-year running mean. The *horizontal dashed lines* indicate mean ± 1σ. The *long horizontal line* represents 21.31 °C, the mean value of 1846–2010. The *short red lines* indicate mean values of each decade, except that the *first short red line* indicates the average value of 1846–1850

Table 2 Statistics of the reconstruction model

Calibration (1960–2011 AD)		Verification (1960–2011 AD)	
		Bootstrap (100 iterations), mean (range)	Jackknife, mean (range)
r	0.68	0.68 (0.50–0.87)	0.68 (0.62–0.71)
R^2	0.47	0.47 (0.25–0.75)	0.47 (0.39–0.51)
R^2_{adj}	0.46	0.46 (0.23–0.74)	0.46 (0.38–0.50)
Standard error of estimate	0.59	0.58 (0.44–0.73)	0.59 (0.55–0.59)
F	43.86	44.10 (16.61–148.48)	43.06 (31.03–50.04)
P	0.0001	0.0001 (0.0001–0.0001)	0.0001 (0.0001–0.0001)

The reconstructed temperature indicated obvious annual- and decadal-scale cold/warm variation. Continuous multi-year high (low) temperatures generally influence the high mountain tree growth more significantly than that of single years. When we defined year with value that exceeded mean $\pm 1\sigma$ as extreme warm/cold year, the extremely cold events lasting over 3 consecutive years were found in 1861–1865, 1896–1898, 1937–1940 and 1967–1971, while there was only one extremely warm event lasting over 3 years during 2000–2005. The 11-year running mean of the reconstructed temperature further disclosed five cold periods (1861–1869, 1889–1899, 1913–1920, 1936–1942, 1952–1990) and three warm periods (1870–1888, 1922–1934, 2000–2005) in the reconstruction. Among them, 1952–1990 was the longest and coldest period and 2000–2005 was the warmest period. In addition, we calculated the mean temperature value of each decade (Fig. 5a), and found that 1960s and 2000s were the coldest and warmest decade since 1846, respectively.

Global warming has been a hot topic during recent decades. The past millennium temperature reconstruction of the Northern Hemisphere revealed evident warming since around 1600, at least since 1850 which has been confirmed by the observation (Christiansen and Ljungqvist 2012; Moberg et al. 2005). However, no secular trend was found in our reconstruction. The distinguishing feature of the reconstruction was the evident warming since 1970, and the rate of warming was about 0.064 °C/year. This warming rate in the Dabie Montains was close to that of the national warming rate since 1984 (0.058 °C/year) (Wang et al. 2010). This recent warming was also captured by other temperature reconstructions in central EC (Fig. 6).

Before the instrumental period, 1865 was recorded as the coldest year in the reconstruction, and 1861–1865 was a 5-year consecutive extremely cold period. According to the historical documents of the last 500 years climate records of Hubei province (Wuhan Central Meteorological Observatory of Hubei Province 1978), Macheng experienced heavy spring snow in 1865. In the same year, rain fell on trees and then froze into ice because the weather was too cold in the nearby Huanggang region. It convincingly confirmed the reliability of our reconstruction.

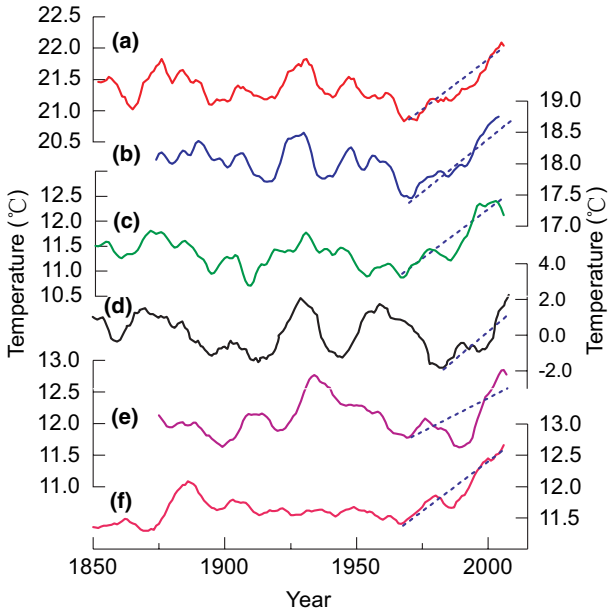

Fig. 6 Temperature comparisons derived from different area of central EC and nearby area. **a** This reconstruction, **b** the mean temperature from February to July by Zheng et al. (2012) and **c** the minimum mean temperature from January to July by Shi et al. (2013) in the Dabie Mountains (DBS), **d** the mean temperature from June to September in Daowushan (DWS), Hunan province by Shi et al. (2015b); **e** the mean temperature from February to June in the eastern Qinling Mountains (EQM) by Chen et al. (2015) and **f** the mean temperature from February to May in the Shennongjia area (SNJ) in central China by Zheng et al. (2016). The *dotted oblique lines* indicate the warming trends. All these records except DWS (**d**) are from the central part of eastern China

3.4 Comparison of different temperature series in central EC and the spatial correlation maps

The reconstructed April–June temperature agreed well with two previous temperature reconstructions in the Dabie Mountains (Fig. 6a–c). At annual scale, the r value between our reconstruction and the February–July mean temperature by Zheng et al. (2012) was 0.68 (1869–2008, $p<0.01$), r was 0.51 (1846–2010, $p<0.01$) for the January–July minimum mean temperature by Shi et al. (2013). For the 11-year running mean series, r was 0.85 and 0.72 at the 99% confidence level, respectively. Moreover, the reconstructed temperature in the Daibie Mountains also indicated synchronous variation with the Daowushan temperature in Hunan province before 1970 (Fig. 6d, Shi et al. 2015b) and the February–June mean temperature in the neighboring eastern Qinling Mountains (Fig. 6e, Chen et al. 2015). Our reconstruction also intermittently agreed with the February–May mean temperature reconstruction

in the Shenongjia area (Fig. 6f, Zheng et al. 2016) at the decadal scale.

The recent warming in all the temperature series of central EC (Fig. 6a–c, e, f) began almost synchronously since 1970 AD. However, it started much later in the Daowushan (DWS) temperature record (Fig. 6d, Shi et al. 2015b). In addition, the warm periods around 1870–1888 and 2000–2005, and the cold periods around 1889–1899 and 1952–1990 in the Daibie Mountains simultaneously appeared in all the other temperature reconstructions in central EC. It is worth noting that the temperature during 1900–1970 in Shennongjia was very stable (Zheng et al. 2016), and no fluctuations of warm or cold periods happened. However, in the Dabie Mountains, the Daowushan and the eastern Qinling Mountains, temperatures were variable and the temperatures were consistently warm around 1922–1934.

Spatial correlation maps demonstrated that the observed temperature showed significantly positive correlations with the homochronous temperatures in most area of China (Fig. 7a), especially significant in the saddle-shaped area between 25–52°N and 82–120°E. The reconstructed temperature also indicated similar correlation pattern, while the most significant areas extended from the study area to its northwest region (Fig. 7b). Moreover, all the r values between the observed/reconstructed temperature in the Dabie Mountains and the April–June mean temperatures from nine other meteorological stations within this significant correlation field (Fig. 7) were statistically significant ($p < 0.01$) (Table 3). r value for the observed temperature ranged from 0.71 to 0.97, and r value for the reconstructed temperature ranged from 0.59 to 0.74 (Table 3), convincingly supported the spatial representativeness of our temperature reconstruction.

Table 3 Correlation coefficient (r) between the observed/reconstructed April–June mean temperature in the Dabie Mountains and the homochronous temperature of each of the nine meteorological stations around the sampling sites over 1951–2010

Stations	Latitude (N)	Longitude (E)	Observation	Reconstruction
Wuhan	30°37′	114°08′	0.97 (n = 52)	0.74 (n = 60)
Xi'an	34°18′	108°56′	0.82 (n = 52)	0.66 (n = 59)
Changsha	28°12′	113°05′	0.71 (n = 52)	0.59 (n = 60)
Hefei	31°47′	117°18′	0.93 (n = 52)	0.70 (n = 58)
Gushi	32°10′	115°37′	0.92 (n = 52)	0.62 (n = 58)
Lushan	29°35′	115°59′	0.86 (n = 52)	0.61 (n = 56)
Liuan	31°45′	116°30′	0.93 (n = 52)	0.67 (n = 55)
Yuncheng	35°03′	111°03′	0.75 (n = 52)	0.62 (n = 55)
Yichang	30°42′	111°18′	0.89 (n = 52)	0.60 (n = 59)

The temperature record of each station started from different year while ended at 2010 consistently. All the r values are significant at the 99% confidence level

3.5 The regional difference of start time of the recent warming in Eastern China

Figure 6a–c, e, f revealed that recent warming in different area of central EC began almost synchronously since 1970 AD. This phenomenon triggered our further thinking about the timing of recent warming in the whole EC. Ideally, it is preferable to compare the same-season or quasi-same season temperature series from EC with the same resolution and evenly geographical distribution. Unfortunately, trees generally response to different climatic factor of different season due to the specific location. This led to the result that the annually resolved temperature reconstructions in EC were comparatively scarce and seasonally

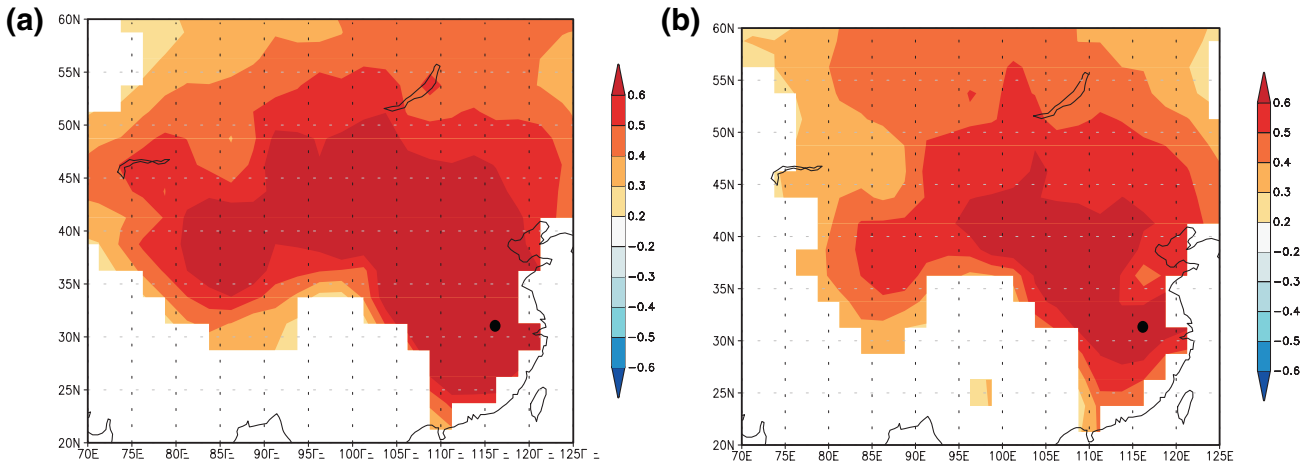

Fig. 7 Correlation of the April–June mean temperature in the Dabie Mountains with the April–June averaged CRU TS3.23 land temperatures through http://climexp.knmi.nl website during 1959–2010. **a** Observation; **b** reconstruction. The *black dot* shows the position of TTZ

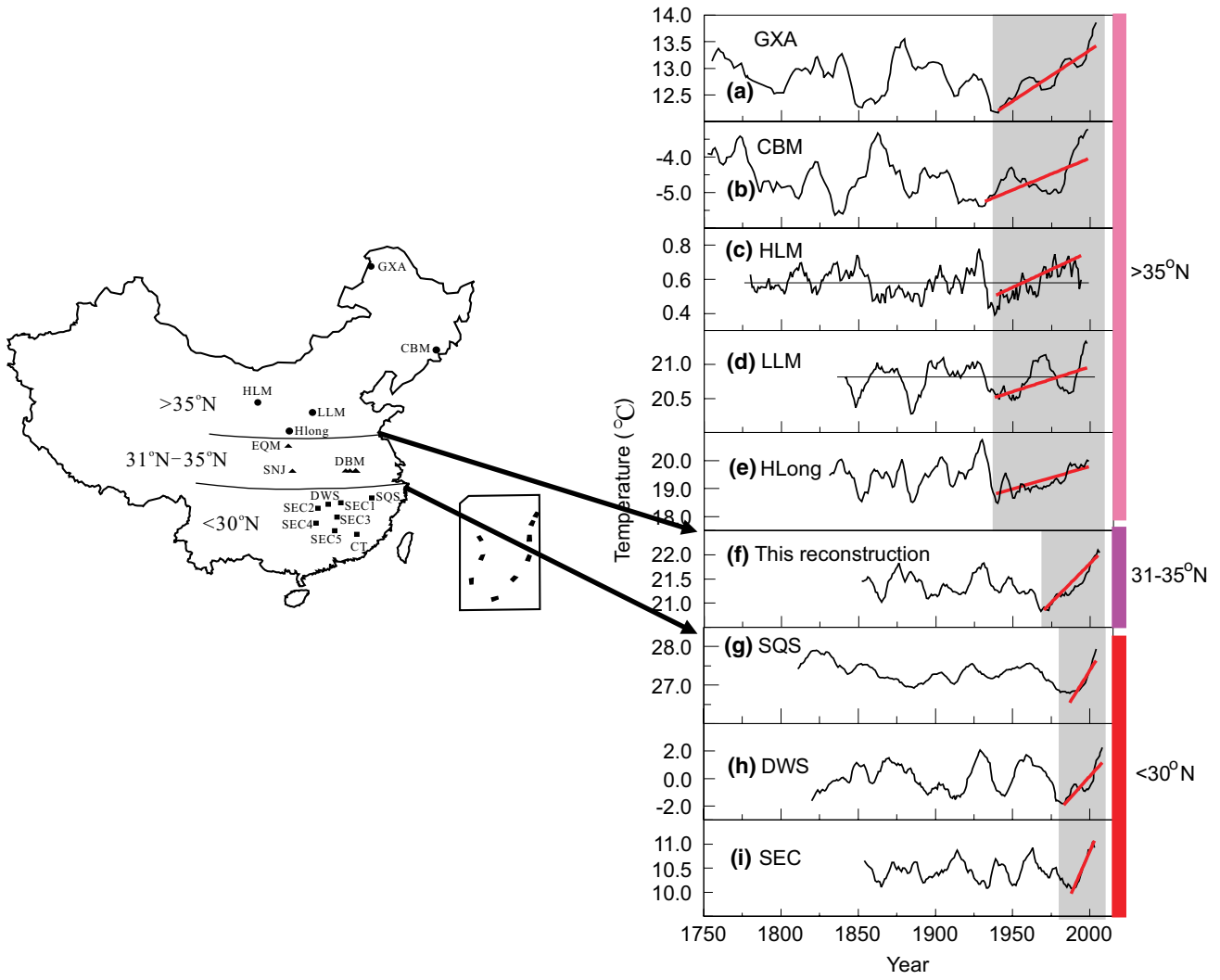

Fig. 8 Comparison of different temperature sequences from the north (>35°N), central (31–35°N) and south (<30°N) part of eastern China (EC). All these temperatures are derived from tree rings. **a** The mean temperature from May to September in the Great Xing'an Mountain (GXA) by Zhang et al. (2011); **b** the mean temperature from February to April in the Changbai Mountain (CBM) by Zhu et al. (2009); **c** the mean temperature from January to August in the Helan Mountain (HLM) by Cai and Liu (2007); **d** the mean temperature from May to July in the Lvliang Mountains (LLM) by Cai et al. (2010); **e** the mean temperature from April to September in the Huanglong Mountain (Hlong) by Cai et al. (2008); **f** this reconstruction; **g** the maximum mean temperature from March to October in the Sanqingshan Mountains (SQS) by Cai and Liu (2017); **h** the mean temperature from June to September in the Daowushan Mountain (DWS) by Shi et al. (2015b); **i** a tree-ring network based January–April temperature over a large spatial scale in southeastern China (SEC: SEC1–SEC5, Duan et al. 2012). More temperature reconstructions from the central part of eastern China please refer to Fig. 6

and regionally uneven. Although previous researches (Cai and Liu 2007; Zheng et al. 2012) believed that different seasonal temperature reconstruction could be used to identify the variability of the annual mean temperature at decadal scale, and the winter-half year temperature has good agreement with the summer time (June–September) temperature variation at decadal scale in EC (Cai et al. 2016). Liu et al. (2009b) found that the winter-half year temperature showed opposite variation with the summer time (May–July) temperature at decadal scale in central China, though both records showed similarly increasing trends since the mid-twentieth century. All in all, there are certain difference for seasonal temperature variations at different time scale (Zhang et al. 2015), we should be cautious about using different seasonal temperature records to represent the same season or annual mean temperature variation, even at the same timescales. Here we could only have a visual comparison of limited tree-ring derived temperature series from EC (Fig. 8).

Although all the temperature series from EC in Fig. 8 were 11-year average smoothed, they demonstrated certain difference, as we discussed above. Neglecting the seasons they represented and the temperatures fluctuations in the early periods of each reconstruction, the

spatial pattern (Fig. 8) indicated that all regions in EC experienced evident warming during recent decades. However, the start time of recent warming in EC was regionally different. It showed an evident north-to-south delay. It started around 1940 AD in the north part of EC (roughly >35°N) (Fig. 8a–e, Chen et al. 2013) or even earlier (Li and Wang 2013; Lyu et al. 2016). In the central part of EC (roughly 31−35°N), it started around 1970 AD (Figs. 6a–c, e, f, 8f). However, it started relatively late in the south part of EC (<30°N), roughly around the 1980s (Fig. 8g–i; Chen et al. 2012b). The result indicated that different regions in EC may have different sensitivity to global warming.

Our result had certain difference with previous researches. Lu et al. (2004) thought that temperature changes occurred almost simultaneously in EC. Chen et al. (2004) and Wang et al. (2010) reported the similar result as ours that the recent warming in EC started earlier in the north part than in the south part. However, Wang et al. (2010) thought it started since the 1970s in the north part (>40°N), while it started since the 1980s in most areas of the south part (<40°N). Chen et al. (2004) found that warming in areas north of 35°N started since the early 1980s, while it started since the late 1980s in areas south of 35°N. The difference of the definitions of the start times and the geographic demarcation of recent warming between our study and previous works (Chen et al. 2004; Wang et al. 2010) was attributable at least in part to the data length used. Our conclusion was based on more than 100 years temperature reconstructions, while their conclusions were based on the short instrumental temperature data (Chen et al. 2004; Wang et al. 2010). Similar researches were reported in other regions of the world. A remarkably northward and north eastward warming was identified in Bangladesh based on the 1971–2010 data (Rahman and Lateh 2016). Majorowicz et al. (2002) found that the start time of recent warming in Canada indicated a systematic delay from east to west. Because of the long-data used, the onset of recent warming in western Canada started with the industrialization, while it was at least one century earlier in eastern Canada. It indicated that data length had important influence on the results of such study.

This work is only the beginning of the discussion about such issue. We should point out that our study was based on very limited temperature series, so we can not rule out other possibilities. We failed to discuss the regional difference of warming intensity in EC for lacking enough same-season temperature reconstructions, not to mention the mechanism. To obtain a robust conclusion about the start time and warming intensity of the recent warming in EC, more temperature data with enough spatial and temporal coverage are needed.

4 Conclusions

We reconstructed the April–June mean temperature in the Dabie Mountains, subtropical eastern China since 1846. The reconstructed temperature had good skill in simulating the observed temperature over the observation period with an explained variance of 46.80%. Five cold (1861–1869, 1889–1899, 1913–1920, 1936–1942 and 1952–1990) and three warm (1870–1888, 1922–1934 and 2000–2005) periods were identified in the reconstruction. We found that the warming trend since 1970 was evident not only in the Dabie Mountains (0.064 °C/year), but also in other areas of eastern China. The spatial and temporal representativeness of our temperature reconstruction was well tested by both the significant spatial correlation patterns and the comparisons with other temperature records in the Dabie Mountains and nearby areas. Based on the tree-ring reconstructed temperatures in eastern China, we found that the start time of the recent warming in eastern China was regional different. It delayed gradually from north to south, starting around 1940 or even earlier in the north part, around 1970 AD in the central part and roughly since the 1980s in the south part.

Acknowledgements This research was the result of the joint funding by the CAS "Light of West China" Program, National Natural Science Foundation of China (41671212, 41171170, 41630531 and 41371221), CAS Key Research Program of Frontier Sciences QYZDJ–SSW–DQC021, the National Basic Research Program (2013CB955903) and the State Key Laboratory of Loess and Quaternary Geology foundation (SKLLQG). The authors appreciate the permission of the Tianma National Nature Reserve Administration Committee for field sampling. We also thank Li Xie and Baofa Shen for helping us in the field trip.

References

Bretherton CS, Widmann M, Dymnikov VP, Wallace JM, Bladé I (1999) The effective number of spatial degrees of freedom of a time-varying field. J Clim 12:1990–2009

Cai QF, Liu Y (2007) January to August temperature variability since 1776 inferred from tree-ring width of *Pinus tabulaeformis* in Helan Mountain. J Geogr Sci 17:293–303

Cai QF, Liu Y (2017) Two centuries temperature variations over subtropical southeast China inferred from *Pinus taiwanensis* Hayata tree-ring width. Clim Dyn 48:1813–1825

Cai QF, Liu Y, Song HM, Sun JY (2008) Tree-ring-based reconstruction of the April to September mean temperature since 1826 AD for north-central Shaanxi Province, China. Sci China Ser D Earth Sci 51(8):1099–1106

Cai QF, Liu Y, Bao G, Lei Y, Sun B (2010) Tree-ring-based May–July mean temperature history for Lüliang Mountains, China, since 1836. Chin Sci Bull 55(26):3008–3014

Cai QF, Liu Y, Lei Y, Bao G, Sun B (2014) Reconstruction of the March–August PDSI since 1703 AD based on tree rings of Chinese pine (*Pinus tabulaeformis* Carr.) in the Lingkong Mountain, southeast Chinese loess Plateau. Clim Past 10:509–521

Cai QF, Liu Y, Wang YC, Ma YY, Liu H (2016) Recent warming evidence inferred from a tree-ring-based winter-half year minimum temperature reconstruction in northwestern Yichang, South Central China, and its relation to the large-scale circulation anomalies. Int J Biometeorol 60:1885–1896. doi:10.1007/s00484-016-1175-2

Campioli M, Gielen B, Göckede M, Papale D, Bouriaud O, Granier A (2011) Temporal variability of the NPP-GPP ratio at seasonal and interannual time scales in a temperate beech forest. Biogeosciences 8:2481–2492

Chen LX, Zhou XJ, Li WL, Luo YF, Zhu WQ (2004) Characteristics of the climate change and its formation mechanism in China in last 80 years. Acta Meteorol Sin 62(5):634–646

Chen F, Yuan YJ, Wei WS, Yu SL, Zhang TW (2012a) Reconstructed temperature for Yong'an, Fujian, Southeast China: linkages to the Pacific Ocean climate variability. Glob Planet Change 86–87:11–19

Chen F, Yuan YJ, Wei WS, Yu SL, Zhang TW (2012b) Tree ring-based winter temperature reconstruction for Changting, Fujian, subtropical region of Southeast China, since 1850: linkages to the Pacific Ocean. Theor Appl Climatol 109 (1–2):141–151

Chen ZJ, Zhang XL, He XY, Davi NK, Cui MX, Peng JJ (2013) Extension of summer (June–August) temperature records for northern Inner Mongolia (1715–2008), China using tree rings. Quat Int 283:21–29

Chen F, Zhang RB, Wang HQ, Qin L (2015) Recent climate warming of central China reflected by temperature-sensitive tree growth in the eastern Qinling Mountains and its linkages to the Pacific and Atlantic Oceans. J Mt Sci 12(2):396–403

Christiansen B (2011) Reconstructing the NH mean temperature: can underestimation of trends and variability be avoided? J Clim 24:674–692

Christiansen B, Ljungqvist FC (2012) The extra-tropical Northern Hemisphere temperature in the last two millennia: reconstructions of low-frequency variability. Clim Past 8:765–786

Christiansen B, Ljungqvist FC (2017) Challenges and perspectives for large-scale temperature reconstructions of the past two millennia. Rev Geophys. doi:10.1002/2016RG000521

Cohen AS, Gergurich EL, Kraemer BM, McGlue MM, McIntyre PB, Russell JM, Simmons JD, Swarzenski PW (2016) Climate warming reduces fish production and benthic habitat in Lake Tanganyika, one of the most biodiverse freshwater ecosystems. PNAS 113(34):9563–9568

Cook ER (1985) A time-series analysis approach to tree-ring standardization. Dissertation for the Doctoral Degree. The University of Arizona, Tucson

Cook ER, Kairiukstis LA (1990) Methods of dendrochronology: applications in the environmental sciences. Kluwer, Dordrecht

Cook ER, Briffa KR, Meko DM, Graybill DA, Funkhouser G (1995) The segment length curse in long tree-ring chronology development for palaeoclimatic studies. Holocene 5:229–235

Crabbe RA, Dash J, Roridguez-Galiano VF, Janous D, Pavelka M, Marek MV (2016) Extreme warm temperatures alter forest phenology and productivity in Europe. Sci Total Environ 563–564:486–495

D'Arrigo R, Jacoby G, Frank D, Pederson N, Cook E, Buckley B, Nachin B, Mijiddorj R, Dugarjav C (2001) 1738 years of Mongolian temperature variability inferred from a tree-ring width chronology of Siberian pine. Geophys Res Lett 28(3):543–546

Davi NK, D'Arrigo RD, Jacoby GC, Cook ER, Anchukaitis KJ, Nachin B, Rao MP, Leland C (2015) A long-term context (931–2005 CE) for rapid warming over Central Asia. Quat Sci Rev 121: 89–97

Duan JP, Zhang QB, Lv LX, Zhang C (2012) Regional-scale winter–spring temperature variability and chilling damage dynamics over the past two centuries in southeastern China. Clim Dyn 39:919–928

Efron B (1979) Bootstrap methods: another look at the jackknife. Ann Stat 7(1):1–26

Esper J, Cook ER, Schweingruber FH (2002) Low frequency signals in long tree-ring chronologies for reconstructing past temperature variability. Science 295:2250–2253

Fritts HC (1976) Tree rings and climate. Academic Press, New York

Gou XH, Chen FH, Yang MX, Jacoby G, Fang KY, Tian QH, Zhang Y (2008) Asymmetric variability between maximum and minimum temperatures in Northeastern Tibetan Plateau: evidence from tree rings. Sci China Ser D Earth Sci 51(1):41–55

Guan YL, Wang RH, Li C, Yao J, Zhang M, Zhao JP (2015) Spatial–temporal characteristics of land surface temperature in Tianshan Mountians area based on MODIS data. Chin J Appl Ecol 26(3):681–688

He Y, Fan GF, Zhang XW, Gao DW, Hu B (2012) Vegetation phenology monitoring and spatio-temporal dynamics in Zhejiang province in past 10 years. Chin Agric Sci Bull 28(16):117–124

Holmes RL (1983) Computer-assisted quality control in tree-ring dating and measurement. Tree Ring Bull 43:69–75

Intergovernmental Panel on Climate Change (IPCC) (2007) Climate change 2007: the physical science basis. Contribution of working group I to the fourth assessment report of the intergovernmental panel on climate change. Cambridge University Press, Cambridge, pp 241–253

Li M, Wang X (2013) Climate-growth relationships of three hardwood species and Korean pine and minimum temperature reconstruction in growing season in Dunhua, China. J Nanjing For Univ Nat Sci Edn 37:29–34

Li LL, Shi JF, Hou XY, Ye JS, Mao HB, Zhao XW, Lu HY (2014) High altitude *Pinus taiwanensis* Hayata growth response to climate in Jiulongshan and Guniujiang, Southeastern China. Chin J Appl Ecol 7:1849–1856

Liang EY, Shao XM, Qin NS (2008) Tree-ring based summer temperature reconstruction for the source region of the Yangtze River on the Tibetan Plateau. Glob Planet Change 61:313–320

Linderholm HW, Björklund J, Seftigen K, Gunnarson BE, Fuentes M (2015) Fennoscandia revisited: a spatially improved tree-ring reconstruction of summer temperatures for the last 900 years. Clim Dyn 45:933–947

Ling HB, Xu HL, Fu J, Zhang QQ, Xu XW (2012) Analysis of temporal–spatial variation characteristics of extreme air temperature in Xinjiang, China. Quat Int 282:14–26

Liu Y, An ZS, Linderholm HW, Chen DL, Song HM, Cai QF, Sun JY, Tian H (2009a) Annual temperatures during the last 2485 years in the mid-eastern Tibetan Plateau inferred from tree rings. Sci China Ser D Earth Sci 52(3):348–359

Liu Y, Linderholm HW, Song HM, Cai QF, Tian QH, Sun JY, Chen DL, Simelton E, Seftigen K, Tian H, Wang RY, Bao G, An ZS (2009b) Temperature variations recorded in *Pinus tabulaeformis* tree rings from the southern and northern slopes of the central Qinling Mountains, central China. Boreas 38(2):285–291

Ljungqvist FC (2010) A new reconstruction of temperature variability in the extra-tropical Northern Hemisphere during the last two millennia. Geogr Ann 92 A(3):339–351

Lu AG, He YQ, Zhang ZL, Pang HX, Gu J (2004) Regional structure of global warming across China during the twentieth century. Clim Res 27:189–195

Lyu SN, Li ZS, Zhang YD, Wang XC (2016) A 414-year tree-ring-based April–July minimum temperature reconstruction and its implications for the extreme climate events, northeast China. Clim Past 12:1879–1888

Majorowicz J, Safanda J, Skinner W (2002) East to west retardation in the onset of the recent warming across Canada inferred from

inversions of temperature logs. J Geophys Res 107(B10):2227. doi:10.1029/2001JB000519
McCarroll D, Loader NJ (2004) Stable isotopes in tree rings. Quat Sci Rev 23:771–801
Melillo JM, Butler SM, Johnson JE, Mohan J, Burton AJ, Zhou Y, Tang J, Steudler PA, Lux H, Burrows E, Vario CL, Hill TD, Bowles F (2011) Changes in the net carbon balance of a forest ecosystem in response to soil warming. PNAS 108(23):9508–9512
Moberg A, Sonechkin DM, Holmgren K, Datsenk NM, Karlén W (2005) Highly variable Northern Hemisphere temperatures reconstructed from low- and high-resolution proxy data. Nature 433:613–617
Ols C, Hofgaard A, Bergeron Y, Drobyshev I (2016) Previous growing season climate controls the occurrence of black spruce growth anomalies in boreal forests of Eastern Canada. Can J For Res 46:696–705
Piovesan G, Biondi F, Di Filippo A, Alessandrini A, Maugeri M (2008) Drought-driven growth reduction in old beech (*Fagus sylvatica* L.) forests of the central Apennines, Italy. Glob Chang Biol 14:1265–1281
Qian W, Qin A (2006) Spatial–temporal characteristics of temperature variation in China. Meteorol Atmos Phys 93: 1–16
Rahman MR, Lateh H (2016) Spatio-temporal analysis of warming in Bangladesh using recent observed temperature data and GIS. Clim Dyn 46:2943–2960
Shao X, Xu Y, Yin Z, Liang E, Zhu H, Wang S (2010) Climatic implications of a 3585-year tree-ring width chronology from the northeastern Qinghai-Tibetan Plateau. Quat Sci Rev 29:2111–2122
Shi JF, Cook ER, Li JB, Lu HY (2013) Unprecedented January–July warming recorded in a 178-year tree-ring width chronology in the Dabie Mountains, southeastern China. Palaeogeogr Palaeocl 381–382:92–97
Shi F, Ge Q, Yang B, Li J, Yang F, Ljungqvist FC, Solomina O, Nakatsuka T, Wang N, Zhao S, Xu C, Fang K, Sano M, Chu G, Fan Z, Gaire NP, Zafar MU (2015a) A multi-proxy reconstruction of spatial and temporal variations in Asian summer temperatures over the last millennium. Clim Chang 13(4):663–676
Shi JF, Li LL, Han ZY, Hou XY, Shi SY (2015b) Tree-ring width based June–September temperature reconstruction and its teleconnection with PDO and ENSO in Mount Daowu, Hunan province. Quat Sci 35(5): 1155–1164 **(in Chinese with English abstract)**
Skomarkova MV, Vaganov EA, Mund M, Knohl A, Linke P, Boerner A, Schulze ED (2006) Inter-annual and seasonal variability of radial growth, wood density and carbon isotope ratios in tree rings of beech (*Fagus sylvatica*) growing in Germany and Italy. Trees 20:571–586
van Oldenborgh GJ, Drijfhout S, van Ulden A, Haarsma R, Sterl A, Severijns C, Hazeleger W, and Dijkstra H (2009) Western Europe is warming much faster than expected. Clim Past 5:1–12
Walther GR, Post E, Convey P, Menzel A, Parmesan C, Beebee TJC, Fromentin JM, Hoegh-Guldberg O, Bairlein F (2002) Ecological responses to recent climate change. Nature 416:389–395
Wang SP, Wang ZH, Piao SL, Fang JY (2010) Regional differences in the timing of recent air warming during the past four decades in China. Chin Sci Bull 55(19):1968–1973
Wang XJ, Gong ZQ, Ren FM, Feng GL (2012) Spatial–temporal characteristics of regional extreme low temperature events in China during 1960–2009. Adv Clim Change Res 3(4):186–194
Wigley TML, Briffa KR, Jones PD (1984) On the average value of correlated time series, with applications in dendroclimatology and hydrometeorology. J Appl Meteorol Clim 23:201–213
Wuhan Central Meteorological Observatory of Hubei Province (1978) Historical climate data of Hubei Province for recent five hundred years, pp 181–182 (**Internal material, in Chinese**)
Xing P, Zhang QB, Lv LX (2014) Absence of late-summer warming trend over the past two and half centuries on the eastern Tibetan Plateau. Glob Planet Change 123:27–35
Yadav RR, Singh J (2002) Tree-ring-based spring temperature patterns over the past four centuries in western Himalaya. Quat Res 57:299–305
Yang B, Kang XC, Bräuning A, Liu J, Qin C, Liu JJ (2010) A 622-year regional temperature history of southeast Tibet derived from tree rings. Holocene 20(2):1–10
Yin ZY, Li MQ, Zhang Y, Shao XM (2016) Growth–climate relationships along an elevation gradient on a southeast-facing mountain slope in the semi-arid eastern Qaidam Basin, northeastern Tibetan Plateau. Trees 30:1095–1109
Yu J, Luo CW, Xu QQ, Meng SW, Li JQ, Liu QJ (2016) Radial growth of *Pinus koraiensis* and carbon sequestration potential of the old growth forest in Changbai Mountain, Northeast China. Acta Ecol Sin 36(9):2626–2636 **(in Chinese with English abstract)**
Zhang XL, He XY, Li JB, Davi N, Chen ZJ, Cui MX, Chen W, Li N (2011) Temperature reconstruction (1750–2008) from Dahurian larch tree-rings in an area subject to permafrost in Inner Mongolia, Northeast China. Clim Res 47:151–159
Zhang QB, Evans MN, Lyu LX (2015) Moisture dipole over the Tibetan Plateau during the past five and a half centuries. Nat Commun 6:8062. doi:10.1038/ncomms9062
Zheng YH, Zhang Y, Shao XM, Yin ZY, Zhang J (2012) Temperature variability inferred from tree-ring widths in the Dabie Mountains of subtropical central China. Trees 26:1887–1894. doi:10.1007/s00468-012-0757-9
Zheng Y, Shao X, Lu F, Li Y (2016) February–May temperature reconstruction based on tree-ring widths of *Abies fargesii* from the Shennongjia area in central China. Int J Biometeorol 60(8):1175–1181
Zhu HF, Fang XQ, Shao XM, Yin ZY (2009) Tree ring-based February–April temperature reconstruction for Changbai Mountain in Northeast China and its implication for East Asian winter monsoon. Clim Past 5:1–6